Title

Olfactory and Neuromodulatory Signals Reverse Visual Object Avoidance to Approach in Drosophila

Journal

Current Biology, 29(12)

ISSN

0960-9822

Authors

Cheng, Karen Y
Colbath, Rachel A
Frye, Mark A

Publication Date

2019-06-01

DOI

10.1016/j.cub.2019.05.010

Peer reviewed

Published in final edited form as:

Curr Biol. 2019 June 17; 29(12): 2058–2065.e2. doi:10.1016/j.cub.2019.05.010.

Olfactory and neuromodulatory signals reverse visual object avoidance to approach in Drosophila

Karen Y. Cheng, **Rachel A. Colbath**, and **Mark A. Frye***

UCLA Department of Integrative Biology and Physiology, University of California, Los Angeles Department of Integrative Biology and Physiology, 610 Charles Young Drive East, Los Angeles, CA 90095-7239, United States

SUMMARY

Behavioral reactions of animals to environmental sensory stimuli are sometimes reflexive and stereotyped, but can also vary depending on contextual conditions. Engaging in active foraging or flight provokes a reversal in the valence of carbon dioxide responses from aversion to approach in *Drosophila* [1,2], whereas mosquitoes encountering this same chemical cue show enhanced approach toward a small visual object [3]. Sensory plasticity in insects has been broadly attributed to the action of biogenic amines, which modulate behaviors such as olfactory learning, aggression, feeding and egg-laying [4–14]. Octopamine acts rapidly upon the onset of flight to modulate the response gain of directionally selective motion-detecting neurons in *Drosophila* [15]. How the action of biogenic amines might couple sensory modalities to each other or to locomotive states remains poorly understood. Here, we use a visual flight simulator [16] equipped for odor delivery [17] to confirm that flies avoid a small contrasting visual object in odorless air [18], but the same animals reverse their preference to approach in the presence of attractive food odor. An aversive odor does not reverse object aversion. Optogenetic activation of either octopaminergic neurons or directionally selective motion detecting neurons that express octopamine receptors elicits visual valence reversal in the absence of odor. Our results suggest a parsimonious model in which odor-activated octopamine release excites the motion detection pathway to increase the saliency of either a small object or a bar, eliciting tracking responses by both visual features.

eTOC blurb

Cheng *et al.* report on a novel multisensory behavior in *Drosophila.* The innate aversion to a small visual object in flight is reversed to approach in an attractive food odor. Object valence reversal can be elicited by optogenetic stimulation of octopaminergic neurons, and requires the activity of columnar directional motion detecting neurons.

*Corresponding Author and Lead Contact: frye@ucla.edu.

AUTHOR CONTRIBUTIONS

Conceptualization, M.A.F. and K.Y.C.; Methodology, M.A.F. and K.Y.C.; Investigation, K.Y.C., R.A.C.; Writing-Original Draft, K.Y.C.; Writing-Review, Revision & Editing, M.A.F.; Funding Acquisition, M.A.F. and K.Y.C.; Resources and Supervision, M.A.F.

DECLARATIONS OF INTERESTS

The authors declare no competing interests.

RESULTS AND DISCUSSION

Visual object valence is reversed by appetitive odor, but not aversive odor

In the presence of odorless air, either flying freely or tethered within a wraparound display of light emitting diodes (LEDs), a fly will steer toward an elongated vertical bar, which likely resembles a landscape feature such as a plant stalk. By contrast, reducing the vertical size of the bar into the shape of a small 'box' likely represents an approaching threat as it evokes a reflexive steering responses oriented away from the visual object [18]. However, a small visual object could represent food or another attractive resource. For mosquitoes flying freely in a wind tunnel, an attractive odor causes animals to approach and land near a small visual object with greater frequency than in clean air [3].

We tested the hypothesis that the odor of apple cider vinegar (ACV), which is highly attractive to *Drosophila* [19–21], modulates the innate behavioral aversion to a small visual object. We equipped the LED arena with an odor delivery nozzle [17] and measured wing steering kinematics in response to a small object oscillating in the visual periphery in the presence or absence of ACV (Figure 1A). Adopting an experimental approach similar to that of Maimon et al. 2008, we presented a 30-degree square object and a 30×94-degree vertical bar (Figure 1B). But, instead of using solid black objects set against a uniform white background [18], we used textured objects set against a textured background to reduce the confound between luminance and motion cues [22]. Steering responses are quantified as the difference between the left and right wing beat amplitude (ΔWBA) encoded by an optical analyzer. Positive values represent steering torque towards the fly's right side and negative values reflect steering towards the left [23]. The bar and object were oscillated at 1 Hz about a point centered 45-degrees to either side of the visual midline (Figure 1C). To facilitate visual inspection of fly steering direction, we plotted time along the vertical axis and ΔWBA on the horizontal axis. We observed similar approach and avoidance responses regardless of which side of the arena the visual stimuli were presented (Figure S1). Therefore, for simplicity, ΔWBA trajectories for stimuli presented on the right side of the arena were multiplied by −1, to reflect them about the visual midline, and pooled with the left-side data. The plot region to the left of visual midline therefore corresponds to responses toward the visual object (Figure 1, approach, blue shading), and *vice versa* for responses oriented opposite the visual object (avoid, gray shading).

Broadly consistent with prior work [18], in odorless air the steering responses of a single wild-type fly are variable - in some trials avoiding and in some trials approaching the small object (Figure 1D). By contrast, the same animal consistently approaches a long vertical bar oscillating at the same azimuthal position (Figure 1D'). Remarkably, upon switching the odor stream from air to ACV, the same fly strongly approaches the small visual object (Figure 1E), and more vigorously approaches the bar (Figure 1E'). A population of 18 animals showed significant reversal from avoidance to approach of the small object in the presence of ACV (Figure 1F,F' $p << 0.01$, Student's paired t-test of ΔWBA steady-state mean of the last two seconds).

This behavioral experiment consists of multiple trials in four different experimental conditions, lasting nearly 10 minutes for each individual. Thus, the visual valence response could have been impacted by classical conditioning, in which a fly might over time associate the small visual object (conditioned stimulus) with a strong, attractive food odorant, ACV (unconditioned stimulus) [24]. To assess this possibility, we plotted mean steering responses over sequential trials and found that object responses were invariant over the duration of the experiment; flies switch to approach the small object within roughly two seconds after the first presentation of ACV (Figure 1G, trial 1). We found no statistical differences between the first and last trial ($p = 0.95$, Student's paired t-test of trial 1 vs. trial 6, Figure 1G). The effect of ACV on reversing the small object valence persists throughout the experiment, rather than building gradually over time.

To examine individual variation of odor-mediated valence reversal behavior, we calculated the endpoint ΔWBA steering responses and compared these measurements before and after ACV presentation for each individual fly (Figure 1H). Each black dot represents the average ΔWBA over the final two seconds in air, and each red dot represents the corresponding mean in ACV for the same animal. The two dots are connected by a blue line if the object valence was reversed by ACV, and by a black line for steering shifts in the same direction. 12 out of 18 flies tested exhibited visual object valence reversal (Figure 1H, blue lines). The inset shows the same plot (with an expanded time axis), but with the dots removed. Each blue line represents a shift from aversion to approach, and the projection on the x-axis indicates the strength of the shift for each individual fly. For 2 out of 18 flies, the steering responses to the small object were not influenced in either direction by ACV (Figure 1H, overlap of black and red dots). By comparison to reversing the valence of the object, ACV further increases the attractiveness of the bar by comparison to the odorless control air stream ($p < 0.01$, Student's paired t-test, Figure 1F'). This was consistent across repeated trials (Figure 1G') and occurred in 10 out of 18 flies tested (Figure 1H').

We next examined whether visual valence reversal by odor persists across fly strain and odorant type. Similar to wild-caught population cage flies (PCF, Figure 1F, F'), OregonR wild-type flies in clean air steer to avoid the small object while robustly approaching the bar (Figure 1I,I'). In the presence of ACV, OregonR flies reverse their steering behavior to approach the small object ($p < 0.01$, Student's paired t-test over final 2-second epoch, Figure 1I). This reversal was observed in 11 out of 13 flies (Figure 1I, inset). Approach toward the bar was unchanged by ACV ($p=0.34$, Figure 1I').

We next tested a different odorant, ethanol (EtOH), which has been shown to be highly attractive in flight [1]. We found that like ACV, EtOH presented to WT-PCF flies reverses the valence of visual object avoidance to approach (Figure 1J, $p< 0.01$). Reversal was observed in 10 out of 13 flies tested (Figure 1J, inset), and the strength of the approach toward the elongated bar was unchanged by EtOH (Figure 1J', $p = 0.07$). By contrast to ACV and EtOH, when tested with benzaldehyde (BA), an odorant that flies actively avoid during flight [25], flies continue to avoid the small object and approach the vertical bar in a manner statistically indistinguishable from their responses in odorless air ($p=0.20$ object; $p=0.23$ bar, Figure 1K,K').

Our results suggest that visual valence reversal is elicited by two highly attractive odorants (ACV and EtOH, Figure 1F & 1J), but not by a canonically aversive odorant (BA, Figure 1K), each delivered at intensities known to evoke stable tracking or avoidance in flight [2,25]. To date, several lines of evidence suggest that attractive and aversive odorants are processed by anatomically segregated olfactory pathways through the mushroom body and lateral horn [26–29]. The mushroom body is classically known for its role in olfactory learning in flies [30], but our analysis suggests that odor-induced visual valence reversal was learning-independent because it has a rapid onset and does not improve with repeated trials (Figure 1G). The lateral horn has been shown to mediate olfactory behaviors in a rapid, experience-independent manner, and also to segregate attractive and aversive odors into anatomical subdomains of the neuropil [26,27,29,31]. Our findings support the hypothesis that the attractive olfactory pathway is specifically engaged for visual object valence reversal [27,28,32].

Optogenetic activation of Tdc2 neurons induces visual valence reversal

To explore how olfactory signals are coupled with visual behaviors, we tested the hypothesis that aminergic neuromodulation is involved in odor-induced visual valence reversal. We expressed Chrimson, a red-shifted excitatory channelrhodopsin [33], in aminergic neurons and modified our experimental paradigm by replacing odor stimulation with 685nm Chrimson-exciting illumination (Figure 1A). The inducible nature of Chrimson allows us to compare each fly's flight steering response before (LED Off) and after (LED On) light-activated membrane depolarization. To account for the slow kinetics of some biogenic amines, we included a 2-minute priming excitation before presenting the visual stimuli. An enhancer-less Gal4 line 'Empty-Gal4' [34] served as a genetic control for transgene expression. Enhancerless controls show behavioral responses to the small object and bar that are similar to those of wild-type flies (Figure 2A,B), although the LED tends to increase approach toward the bar ($p=0.054$, Figure 2B'). Remarkably, in the absence of odor, optogenetic depolarization of octopaminergic/tyraminergic neurons by the Tdc2-Gal4 driver [35] reverses the steering responses to the small object from aversion to approach, while also increasing the steering responses toward the bar (Figure 2C, Fig S2C, *** $p << 0.01$, Student's paired t-test). 15 out of the 16 flies tested showed valence reversal upon Tdc2>Chrimson activation (Figure 2C, inset). By contrast, optogenetic activation of dopaminergic neurons (TH>Chrimson, Figure 2D, $p=0.956$), mushroom-body specific dopaminergic neurons (PAM>Chrimson, Figure 2E, $p=0.045$), or serotonergic neurons (TRH>Chrimson, Figure 2F, $p=0.866$) failed to evoke visual valence reversal. The difference in steering amplitude of object responses to LED On and LED Off by PAM>Chrimson was statistically significant, but activating these neurons merely weakened the small object avoidance without reversing it (Figure 2E).

Depolarizing Tdc2-labeled neurons is sufficient to robustly induce visual valence reversal in the absence of appetitive odor in a flying fly (Figure 2C). Tdc2-Gal4 labels both octopaminergic (OA) and tyraminergic (TA) neurons. Indirect evidence implicates OA, as the two amines have antagonistic effects [36] and exert opposite effects on cAMP and Ca^{2+} concentrations downstream of the cognate G-protein coupled receptors [37]. OA has been implicated in gain modulation in every visual neuron studied [15,38–41]. Another important

issue is the circuit mechanisms that stimulate Tdc2 neurons are unknown. Our lab previously reported calcium response increases in Tdc2 neurons increased upon the presentation of ACV in quiescent flies [42]. Other work has demonstrated that Tdc2 neurons in larvae are activated upon optogenetic excitation of Orco [43], a broadly expressed olfactory co-receptor [44]. Identifying the specific circuitry and neuronal subdomains of Tdc2 neurons that are activated by attractive odorants, and the specificity of OA signaling, requires further investigation.

T4/T5 motion detectors are necessary for object aversion and sufficient to induce visual valence reversal

We assessed the synaptic organization of Tdc2 neurons in the optic lobe by co-labeling with DenMark [45] and synaptotagmin [46]. Consistent with previous findings [47], we found that Tdc2 neurons are broadly presynaptic in the optic lobe, showing strong and broadly distributed *syt* labeling throughout the medulla and lobula complex (Figure 3A). We found dense DenMark labeling within the central brain and subesophageal zone, but not within the optic lobe lamina (Figure 3A).

We next sought to identify Tdc2 targets in the optic lobe that could mediate odor-induced object valence reversal. Behavioral responses to visual objects are mediated by the superposition of directional motion signals and higher-order non-directional signals [48–50], and neither system alone is sufficient to drive the full complement of normal behaviors [51–54]. Identified neurons of the directionally selective motion detection system have been shown to be modulated by octopamine. In particular, several wide-field integration neurons of the third optic ganglion that control optomotor behavior [42] exhibit Tdc2-dependent increases in visual response gain upon flight initiation [15,43,44], and one has been shown to be modulated by odor [38]. Presynaptic inputs to the lobula plate, small-field T4 and T5 motion detectors, comprise the first stage of visual processing in which directional selectivity arises in individual cells, and express OA receptors albeit at a relatively low level by comparison to other aminergic receptors [55]. Presynaptic inputs to T4/T5 neurons are also modulated by OA [40].

We tested the hypothesis that optogenetic activation of T4/T5 reverses the valence of object responses. We expressed Chrimson in T4/T5 neurons and subjected these flies to our visual optogenetics behavioral paradigm, but without the 2-minute priming excitation used in the Tdc2>Chrimson experiment because T4/T5 have rapid response kinetics (see Methods). Transgenic control animals showed qualitatively normal albeit slightly smaller amplitude object avoidance and bar tracking responses (Figure 3B,B’), neither of which were influenced by the LED stimulus (Figure 3B,B’). By contrast, optogenetically activating T4/T5 neurons mimicked the influence of both appetitive odor and Tdc2>Chrimson in all 18 flies we tested ($p << 0.01$, Figure 3C,C’).

Since T4/T5 neurites innervate four layers of the lobula plate that each represent a separate cardinal direction of motion [56,57], one might expect that optogenetically depolarizing the full population of directionally tuned T4 and T5 small-field motion detecting neurons would render flies unable to perceive and respond to directional motion cues. Indeed, when we increased the LED intensity 4-fold from 0.010 mW/mm^2 to 0.040 mW/mm^2, we observed

diminished approach behavior to both the small object and vertical bar (Figure S3A,A'), as well as diminished wide-field optomotor responses (Figure S3A"). These results show that mild T4/T5 depolarization is sufficient to induce visual valence reversal from avoidance to approach toward the small object (Figure 3C), while strengthening approach toward the bar (Figure 3C'), responses that are qualitatively similar to the effects of ACV or EtOH (Figure 1F,F', 1J,J'). These results corroborate recent work showing that appropriately tuned Chrimson excitation can enhance the cellular responses to visual stimuli [58].

We next examined the effect on visual valence reversal when T4/T5 neurons were chronically hyperpolarized with Kir2.1. By contrast to the normal responses by genetic controls (Figure 3D,D'), flies with hyperpolarized T4/T5 neurons show essentially no steering responses to the moving object (Figure 3E), and diminished bar approach that was nevertheless significantly enhanced by odor ($p<0.01$, Figure 3E'). These results indicate that directional motion detectors play a crucial role in behavioral responses to moving objects and bars, yet odor modulation persists qualitatively when the performance of these cells is reduced.

T4/T5 activity is both necessary and sufficient for behavioral approach toward moving objects during flight (Figure 3). How might T4/T5 neurons participate in object aversion in clean air as well object tracking in odor? It has previously been posited that the neural circuits involved in object classification may have overlapping cellular components [18]. T4/T5 neurons have been broadly implicated in bar tracking behaviors [22,52,53] as well as object-dependent male courtship behavior [50]. Thus, it stands to reason that T4/T5 may supply local motion information to many different visual circuits. Recent work has characterized several classes of columnar projection neurons (VPN) that encode visual features such as looming [59], movement of small contrasting targets [60], and optical disparities generated by the vertical edges of bar stimuli [61]. These cell types are postsynaptic in the lobula, but local trans-lobula plate neurons with dendrites in the lobula-plate and terminals in the lobula could convey directional motion signals to feature-based processes [62,63].

Octopaminergic neuromodulation of visual processing is hierarchical

Pharmacological delivery of OA (or an agonist), and induced excitation or chronic silencing of Tdc2 combine to demonstrate that Tdc2 release of OA modulates virtually every visual processing neuron so far tested. We therefore cannot determine whether the phenocopy of odor results (Figure 1) by optogenetic excitation of Tdc2 neurons (Figure 2) or T4/T5 neurons (Figure 3) is linked by causality or coincidence. Tdc2 activity might be increasing the response gain of upstream columnar inputs to T4/T5, which could be functionally equivalent to optogenetically increasing the response gain in T4/T5. We attempted to assess this issue by targeting RNAi against OA receptor genes specifically within T4/T5 neurons, but the genetic controls failed to show normal visual behavior (data not shown). Further analysis using more robust reagents will be required to discover specifically the visual neurons at the crux of odor or OA mediated visual valence reversal behavior.

An important aspect of our findings is that all behavioral manipulations were performed with animals in active flight. The transition from quiescence to active flight or walking

behavior in *Drosophila* is associated with increased response gain of and shifted frequency tuning by wide-field neurons of the lobula plate [15,40,64–66]. The modulatory influence by locomotor state has been shown to depend upon the activity of Tdc2 neurons [15,64]. We posit that odor-evoked octopaminergic modulation of visual valence behavior implicates a hierarchy of OA neuromodulation, because this behavior is apparently superimposed upon the neuromodulation on motion vision driven by the onset of locomotion. In other words, OA modulation of motion vision circuitry triggered by the onset of active flight is by itself insufficient to trigger visual valence reversal (Figure 1). Rather, the presentation of either an appetitive odorant or Tdc2 optogenetic activation in an already flying animal is required to induce visual valence reversal (Figure 1F & 2C). Such a hierarchy could explain why ACV failed to modulate visual responses by T4/T5 neurons in a quiescent imaging preparation [42].

Given the diverse neuronal morphologies contained within the ensemble of Tdc2-Gal4 positive neurons [47,67], it seems highly unlikely that all Tdc2 cells function as a single ‘mega-interneuron’. Hierarchical OA neuromodulation by behavioral state and cross-modal sensory activation is more likely to be mediated by the recruitment of distinct subpopulations of Tdc2 neurons, or by differences in the distribution and molecular action of the various OA receptor types, or both [68]. Indeed, recent work has shown that, depending on experimental parameters, activation of Tdc2 neurons can decrease song behaviors [69] or promote male-to-male courtship [6], demonstrating the functional diversity of Tdc2 action.

CONCLUSIONS

In this study we characterized a novel behavior of *Drosophila melanogaster,* odor-induced visual valence reversal. Taken together, our results implicate a conceptual model for multisensory processing (Figure 4) in which an appetitive odor stimulates Tdc2 release that increases the response gain of the motion vision pathway. This excitatory modulation and the interaction between the motion and object vision pathways somehow induce object approach behavior. T4/T5 motion detectors might affect the object vision pathway via TLP neurons. What remains to be determined is how Tdc2 neurons of the optic lobe are driven by the olfactory system, how Tdc2 neurons interact with T4/T5 motion detectors or pre- and postsynaptic pathways, as well as the underlying circuitry for avoidance of a small moving object, which in the presence of food odor is overridden by approach toward the object.

STAR METHODS

CONTACT FOR REAGENT AND RESOURCE SHARING

Further information and requests for reagents can be requested from the corresponding author, Mark A. Frye (frye@ucla.edu).

EXPERIMENTAL MODEL AND SUBJECT DETAILS

All *Drosophila melanogaster*were maintained in a humidity-controlled environment on a 12:12 hour circadian light:dark cycle. Crosses involving aminergic cell types were raised at 18°C (Tritech Research) to reduce Gal4 toxicity. All other flies were raised in a 25°C animal

room. For behavior experiments, female flies 3-5 days posteclosion were used, and experiments are conducted within 4 hours after lights-on or within 4 hours prior to lights-off.

METHOD DETAILS

Rigid tether flight simulator and odor delivery—The rigid tether visual arena is previously described [18]. The arena comprises of computer-controlled 96×32 pixel array of 570nm LEDs arranged in a cylinder, each pixel subtending 3.75 degrees on the retina at the azimuth. Experimental flies were cold-anesthetized and tethered to 0.1mm-diameter tungsten pins. Flies were allowed to recover for one hour after tethering in a plastic box containing a dish of water and illuminated by a heat lamp to maintain humidity. In the flight arena, an infrared emitter and sensor are placed above and below the tethered fly to capture a shadow of the beating wings on the sensor (Figure 1A). The sensor and associated electronics measure the amplitude of each wing beat. The difference in amplitude of the left and right wing signals (ΔWBA) is proportional to yaw torque [23] and indicates the fly's attempt to steer left (ΔWBA<0) or right (ΔWBA>0).

The following visual stimuli are used in all behavioral paradigms: a 30 degree, randomly textured square, and an elongated, textured bar subtending 30 degrees in width and 94 degrees in height at the eye (Figure 1B). Visual stimuli are presented in random order on the left or right 45-degrees from midline (Figure 1C). The stimuli oscillate via a 1Hz sine wave with an amplitude of 15 degrees. Each experimental condition (object/bar, arena left/right) is presented 4-6 times. Trials in clean air are presented before the odor-paired trials rather than being interspersed in order to limit potential effects of olfactory working memory [70]. A closed loop bar fixation trial is placed between open-loop test trials to keep the fly actively engaged in the experiment.

Odors used in this study were apple cider vinegar (Ralph's Grocery generic brand), ethanol diluted to 70% and benzaldehyde diluted to 40%. Because benzaldehyde precipitates easily, the odorant is placed on filter paper inside the odor delivery tube [25]. Odor delivery to the tethered fly has been described previously [17]. Briefly, saturated odor vapor was delivered through a pipet tip placed 1 cm in front of the fly's head and drawn away by vacuum in a tube positioned behind the fly. To confirm that each fly responded to the odor, we administered a 5-second odor response test without visual cues, and only included flies in the experiment that showed a significant increase in wingbeat frequency upon the onset of the odor pulse [71]. No flies were run more than once. At the beginning of each experiment day, a photoionization detector, was used to confirm the ON/OFF switching of air/odor at the location of the tethered fly.

Rigid flight simulator and optogenetic activation—Optogenetics flight experiments are conducted in a similar setup to the odor experiments, except that blue LED panels (470nm) are used instead of green LED panels (570nm) to avoid Chrimson activation by the display [33]. To reduce the illumination intensity, three layers of neutral density filter were placed over the LED display. The odor delivery system is replaced by a red LED (685nm) that illuminates the entire fly. Similar to the odor experiment paradigm, all LED Off trials

were conducted first, followed by the block of LED On trials. The same visual patterns from the odor experiments were used and presented with a random block experimental design.

For flies expressing aminergic drivers, a 2-minute closed loop fixation period with the LED On is placed between the LED Off and LED On blocks. This was done to account for the slow kinetics of activation of biogenic amines reported in the literature, which predominantly mediate their effects via G-protein coupled receptors [72]. For flies expressing Chrimson under the control of Empty-splitGal4 and T4/T5-splitGal4, the 2-minute 'preincubation' LED On period is removed, and the LED is turned off in between trials during the LED On block. Except for the high-intensity experiment (Supp Figure 3C–C"), all optogenetics experiments used a LED power intensity of 10μW/mm^2. Power intensity was increased to 40μW/mm^2 for the high-intensity experiment.

All-trans-retinal—For proper Chrimson protein conformation, all-trans-retinal is required. Though flies endogenously produce retinal, additional ATR is added to the food to boost performance [73]. F1 Chrimson flies are raised in 0.5mM ATR food post-eclosion for at least 3 and no more than 5 days before being used for experiments.

QUANTIFICATION AND STATISTICAL ANALYSIS

Student's paired t-test of the last two seconds was performed in MATLAB 2017a (MathWorks, Inc.) to compare mean epoch ΔWBA.

DATA AND SOFTWARE AVAILABILITY

Data and code from this manuscript are available upon request from the corresponding author, Mark A. Frye (frye@ucla.edu)

Supplementary Material

Refer to Web version on PubMed Central for supplementary material.

ACKNOWLEDGMENTS

We thank Dr. Ben Hardcastle for technical assistance and advice, and Dr. Mehmet Keleş for reagents and advice. This work was supported by grants from the National Science Foundation (IOS-1455869) to M.A.F. and National Institutes of Health (F31-EY029599) to K.Y.C.

REFERENCES

1. van Breugel F, Huda A, and Dickinson MH (2018). Distinct activity-gated pathways mediate attraction and aversion to CO2 in Drosophila. Nature 564, 420–424. [PubMed: 30464346]
2. Wasserman S, Salomon A, and Frye MA (2013). Drosophila tracks carbon dioxide in flight. Curr. Biol. 23, 301–306. [PubMed: 23352695]
3. van Breugel F, Riffell J, Fairhall A, and Dickinson MH (2015). Mosquitoes Use Vision to Associate Odor Plumes with Thermal Targets. Curr. Biol. 25, 2123–2129. [PubMed: 26190071]
4. Keene AC, and Waddell S (2007). Drosophila olfactory memory: single genes to complex neural circuits. Nat. Rev. Neurosci. 8, 341–354. [PubMed: 17453015]
5. Kim SM, Su C-Y, and Wang JW (2017). Neuromodulation of Innate Behaviors in Drosophila. Annu. Rev. Neurosci. 40, 327–348. [PubMed: 28441115]

6. Certel SJ, Savella MG, Schlegel DCF, and Kravitz EA (2007). Modulation of Drosophila male behavioral choice. Proc. Natl. Acad. Sci. U. S. A. 104, 4706–4711. [PubMed: 17360588]
7. Dierick HA, and Greenspan RJ (2007). Serotonin and neuropeptide F have opposite modulatory effects on fly aggression. Nat. Genet. 39, 678–682. [PubMed: 17450142]
8. Inagaki HK, Ben-Tabou de-Leon S, Wong AM, Jagadish S, Ishimoto H, Barnea G, Kitamoto T, Axel R, and Anderson DJ (2012). Visualizing neuromodulation in vivo: TANGO-mapping of dopamine signaling reveals appetite control of sugar sensing. Cell 148, 583–595. [PubMed: 22304923]
9. Inagaki HK, Jung Y, Hoopfer ED, Wong AM, Mishra N, Lin JY, Tsien RY, and Anderson DJ (2014). Optogenetic control of Drosophila using a red-shifted channelrhodopsin reveals experience-dependent influences on courtship. Nat. Methods 11, 325–332. [PubMed: 24363022]
10. Alekseyenko OV, Chan Y-B, Li R, and Kravitz EA (2013). Single dopaminergic neurons that modulate aggression in Drosophila. Proc. Natl. Acad. Sci. U. S. A. 110, 6151–6156. [PubMed: 23530210]
11. Alekseyenko OV, Chan Y-B, Fernandez M de la P, Bülow T, Pankratz MJ, and Kravitz EA (2014). Single serotonergic neurons that modulate aggression in Drosophila. Curr. Biol. 24, 2700–2707. [PubMed: 25447998]
12. Zhou C, Rao Y, and Rao Y (2008). A subset of octopaminergic neurons are important for Drosophila aggression. Nat. Neurosci. 11, 1059–1067. [PubMed: 19160504]
13. Zhou C, Huang H, Kim SM, Lin H, Meng X, Han K-A, Chiang A-S, Wang JW, Jiao R, and Rao Y (2012). Molecular genetic analysis of sexual rejection: roles of octopamine and its receptor OAMB in Drosophila courtship conditioning. J. Neurosci. 32, 14281–14287. [PubMed: 23055498]
14. Rezával C, Nojima T, Neville MC, Lin AC, and Goodwin SF (2014). Sexually dimorphic octopaminergic neurons modulate female postmating behaviors in Drosophila. Curr. Biol. 24, 725–730. [PubMed: 24631243]
15. Suver MP, Mamiya A, and Dickinson MH (2012). Octopamine neurons mediate flight-induced modulation of visual processing in Drosophila. Curr. Biol. 22, 2294–2302. [PubMed: 23142045]
16. Reiser MB, and Dickinson MH (2008). A modular display system for insect behavioral neuroscience. J. Neurosci. Methods 167, 127–139. [PubMed: 17854905]
17. Chow DM, and Frye MA (2008). Context-dependent olfactory enhancement of optomotor flight control in Drosophila. J. Exp. Biol. 211, 2478–2485. [PubMed: 18626082]
18. Maimon G, Straw AD, and Dickinson MH (2008). A simple vision-based algorithm for decision making in flying Drosophila. Curr. Biol. 18, 464–470. [PubMed: 18342508]
19. Budick SA, and Dickinson MH (2006). Free-flight responses of Drosophila melanogaster to attractive odors. J. Exp. Biol. 209, 3001–3017. [PubMed: 16857884]
20. Duistermars BJ, Chow DM, and Frye MA (2009). Flies require bilateral sensory input to track odor gradients in flight. Curr. Biol. 19, 1301–1307. [PubMed: 19576769]
21. Semmelhack JL, and Wang JW (2009). Select Drosophila glomeruli mediate innate olfactory attraction and aversion. Nature 459, 218–223. [PubMed: 19396157]
22. Keleş MF, Mongeau J-M, and Frye MA (2019). Object features and T4/T5 motion detectors modulate the dynamics of bar tracking by Drosophila. J. Exp. Biol. 222,190017.
23. Tammero LF, Frye MA, and Dickinson MH (2004). Spatial organization of visuomotor reflexes in Drosophila. J. Exp. Biol. 207, 113–122. [PubMed: 14638838]
24. Pavlov PI (2010). Conditioned reflexes: An investigation of the physiological activity of the cerebral cortex. Ann Neurosci 17, 136–141. [PubMed: 25205891]
25. Wasserman S, Lu P, Aptekar JW, and Frye MA (2012). Flies dynamically anti-track, rather than ballistically escape, aversive odor during flight. J. Exp. Biol. 215, 2833–2840. [PubMed: 22837456]
26. Grabe V, and Sachse S (2018). Fundamental principles of the olfactory code. Biosystems. 164, 94–101. [PubMed: 29054468]
27. Sachse S, and Beshel J (2016). The good, the bad, and the hungry: how the central brain codes odor valence to facilitate food approach in Drosophila. Curr. Opin. Neurobiol. 40, 53–58. [PubMed: 27393869]

28. Masse NY, Turner GC, and Jefferis GSXE (2009). Olfactory information processing in Drosophila. Curr. Biol. 19, R700–13. [PubMed: 19706282]
29. Schultzhaus JN, Saleem S, Iftikhar H, and Carney GE (2017). The role of the Drosophila lateral horn in olfactory information processing and behavioral response. J. Insect Physiol. 98, 29–37. [PubMed: 27871975]
30. de Belle JS, and Heisenberg M (1994). Associative odor learning in Drosophila abolished by chemical ablation of mushroom bodies. Science 263, 692–695. [PubMed: 8303280]
31. Fişek M, and Wilson RI (2014). Stereotyped connectivity and computations in higher-order olfactory neurons. Nat. Neurosci. 17, 280–288. [PubMed: 24362761]
32. Strutz A, Soelter J, Baschwitz A, Farhan A, Grabe V, Rybak J, Knaden M, Schmuker M, Hansson BS, and Sachse S (2014). Decoding odor quality and intensity in the Drosophila brain. Elife 3, e04147. [PubMed: 25512254]
33. Klapoetke NC, Murata Y, Kim SS, Pulver SR, Birdsey-Benson A, Cho YK, Morimoto TK, Chuong AS, Carpenter EJ, Tian Z, et al. (2014). Independent optical excitation of distinct neural populations. Nat. Methods 11, 338–346. [PubMed: 24509633]
34. Hampel S, McKellar CE, Simpson JH, and Seeds AM (2017). Simultaneous activation of parallel sensory pathways promotes a grooming sequence in Drosophila. Elife 6, 28804.
35. Cole SH, Carney GE, McClung CA, Willard SS, Taylor BJ, and Hirsh J (2005). Two functional but noncomplementing Drosophila tyrosine decarboxylase genes: distinct roles for neural tyramine and octopamine in female fertility. J. Biol. Chem. 280, 14948–14955. [PubMed: 15691831]
36. Saraswati S, Fox LE, Soll DR, and Wu C-F (2004). Tyramine and octopamine have opposite effects on the locomotion of Drosophila larvae. J. Neurobiol. 58, 425–441. [PubMed: 14978721]
37. Roeder T (2005). Tyramine and octopamine: ruling behavior and metabolism. Annu. Rev. Entomol. 50, 447–477. [PubMed: 15355245]
38. Longden KD, and Krapp HG (2010). Octopaminergic modulation of temporal frequency coding in an identified optic flow-processing interneuron. Front. Syst. Neurosci. 4, 153. [PubMed: 21152339]
39. de Haan R, Lee Y-J, and Nordström K (2012). Octopaminergic modulation of contrast sensitivity. Front. Integr. Neurosci. 6, 55. [PubMed: 22876224]
40. Arenz A, Drews MS, Richter FG, Ammer G, and Borst A (2017). The Temporal Tuning of the Drosophila Motion Detectors Is Determined by the Dynamics of Their Input Elements. Curr. Biol. 27, 929–944. [PubMed: 28343964]
41. Creamer MS, Mano O, and Clark DA (2018). Visual Control of Walking Speed in Drosophila. Neuron 100, 1460–1473.e6. [PubMed: 30415994]
42. Wasserman SM, Aptekar JW, Lu P, Nguyen J, Wang AL, Keles MF, Grygoruk A, Krantz DE, Larsen C, and Frye MA (2015). Olfactory neuromodulation of motion vision circuitry in Drosophila. Curr. Biol. 25, 467–472. [PubMed: 25619767]
43. Ma Z, Stork T, Bergles DE, and Freeman MR (2016). Neuromodulators signal through astrocytes to alter neural circuit activity and behaviour. Nature 539, 428–432. [PubMed: 27828941]
44. Larsson MC, Domingos AI, Jones WD, Chiappe ME, Amrein H, and Vosshall LB (2004). Or83b encodes a broadly expressed odorant receptor essential for Drosophila olfaction. Neuron 43, 703–714. [PubMed: 15339651]
45. Nicolaï LJJ, Ramaekers A, Raemaekers T, Drozdzecki A, Mauss AS, Yan J, Landgraf M, Annaert W, and Hassan BA (2010). Genetically encoded dendritic marker sheds light on neuronal connectivity in Drosophila. Proc. Natl. Acad. Sci. U. S. A. 107, 20553–20558. [PubMed: 21059961]
46. Zhang YQ, Rodesch CK, and Broadie K (2002). Living synaptic vesicle marker: synaptotagmin-GFP. Genesis 34, 142–145. [PubMed: 12324970]
47. Busch S, Selcho M, Ito K, and Tanimoto H (2009). A map of octopaminergic neurons in the Drosophila brain. J. Comp. Neurol. 513, 643–667. [PubMed: 19235225]
48. Theobald JC, Duistermars BJ, Ringach DL, and Frye MA (2008). Flies see second-order motion. Curr. Biol. 18, R464–5. [PubMed: 18522814]
49. Theobald JC, Shoemaker PA, Ringach DL, and Frye MA (2010). Theta motion processing in fruit flies. Front. Behav. Neurosci. 4, 00035.

50. Ribeiro IMA, Drews M, Bahl A, Machacek C, Borst A, and Dickson BJ (2018). Visual Projection Neurons Mediating Directed Courtship in Drosophila. Cell 174, 607–621.e18. [PubMed: 30033367]
51. Aptekar JW, Shoemaker PA, and Frye MA (2012). Figure tracking by flies is supported by parallel visual streams. Curr. Biol. 22, 482–487. [PubMed: 22386313]
52. Bahl A, Ammer G, Schilling T, and Borst A (2013). Object tracking in motion-blind flies. Nat. Neurosci. 16, 730–738. [PubMed: 23624513]
53. Fenk LM, Poehlmann A, and Straw AD (2014). Asymmetric processing of visual motion for simultaneous object and background responses. Curr. Biol. 24, 2913–2919. [PubMed: 25454785]
54. Bahl A, Serbe E, Meier M, Ammer G, and Borst A (2015). Neural Mechanisms for Drosophila Contrast Vision. Neuron 88, 1240–1252. [PubMed: 26673659]
55. Pankova K, and Borst A (2016). RNA-Seq Transcriptome Analysis of Direction-Selective T4/T5 Neurons in Drosophila. PLoS One 11, e0163986. [PubMed: 27684367]
56. Maisak MS, Haag J, Ammer G, Serbe E, Meier M, Leonhardt A, Schilling T, Bahl A, Rubin GM, Nern A, et al. (2013). A directional tuning map of Drosophila elementary motion detectors. Nature 500, 212–216. [PubMed: 23925246]
57. Mauss AS, Meier M, Serbe E, and Borst A (2014). Optogenetic and pharmacologic dissection of feedforward inhibition in Drosophila motion vision. J. Neurosci. 34, 2254–2263. [PubMed: 24501364]
58. Busch C, Borst A, and Mauss AS (2018). Bi-directional Control of Walking Behavior by Horizontal Optic Flow Sensors. Curr. Biol. 28, 4037–4045.e5. [PubMed: 30528583]
59. Namiki S, Dickinson MH, Wong AM, Korff W, and Card GM (2018). The functional organization of descending sensory-motor pathways in Drosophila. Elife 7, 34272.
60. Keleş MF, and Frye MA (2017). Object-Detecting Neurons in Drosophila. Curr. Biol. 27, 680–687. [PubMed: 28190726]
61. Aptekar JW, Keleş MF, Lu PM, Zolotova NM, and Frye MA (2015). Neurons Forming Optic Glomeruli Compute Figure-Ground Discriminations in Drosophila. J. Neurosci. 35, 7587–7599. [PubMed: 25972183]
62. Raghu SV, and Borst A (2011). Candidate glutamatergic neurons in the visual system of Drosophila. PLoS One 6, e19472. [PubMed: 21573163]
63. Fischbach K-F, and Dittrich APM (1989). The optic lobe of Drosophila melanogaster. I. A Golgi analysis of wild-type structure. Cell Tissue Res. 258, 441–475.
64. Maimon G, Straw AD, and Dickinson MH (2010). Active flight increases the gain of visual motion processing in Drosophila. Nat. Neurosci. 13, 393–399. [PubMed: 20154683]
65. Chiappe ME, Seelig JD, Reiser MB, and Jayaraman V (2010). Walking modulates speed sensitivity in Drosophila motion vision. Curr. Biol. 20, 1470–1475. [PubMed: 20655222]
66. Jung SN, Borst A, and Haag J (2011). Flight activity alters velocity tuning of fly motion-sensitive neurons. J. Neurosci. 31, 9231–9237. [PubMed: 21697373]
67. Claßen G, and Scholz H (2018). Octopamine Shifts the Behavioral Response From Indecision to Approach or Aversion in Drosophila melanogaster. Front. Behav. Neurosci. 12, 131. [PubMed: 30018540]
68. Farooqui T (2012). Review of octopamine in insect nervous systems. Open access insect physiol. 4, 1–17.
69. O'Sullivan A, Lindsay T, Prudnikova A, Erdi B, Dickinson M, and von Philipsborn AC (2018). Multifunctional Wing Motor Control of Song and Flight. Curr. Biol. 28, 2705–2717.e4. [PubMed: 30146152]
70. Saxena N, Natesan D, and Sane SP (2018). Odor source localization in complex visual environments by fruit flies. J. Exp. Biol. 221,172023.
71. Chow DM, Theobald JC, and Frye MA (2011). An olfactory circuit increases the fidelity of visual behavior. J. Neurosci. 31, 15035–15047. [PubMed: 22016537]
72. Monastirioti M, Gorczyca M, Rapus J, Eckert M, White K, and Budnik V (1995). Octopamine immunoreactivity in the fruit fly Drosophila melanogaster. J. Comp. Neurol. 356, 275–287. [PubMed: 7629319]

73. Simpson JH, and Looger LL (2018). Functional Imaging and Optogenetics in Drosophila. Genetics 208, 1291–1309. [PubMed: 29618589]

74. von Reyn CR, Nern A, Williamson WR, Breads P, Wu M, Namiki S, Card GM Feature integration drives probabilistic behavior in the Drosophila escape response Neuron, 94 (2017), pp. 1190–1204 [PubMed: 28641115]

Highlights

- A fly's innate aversion to a small visual object is reversed by odor
- Object valence is reversed by attractive odors, but not an aversive one
- Activating octopaminergic neurons is sufficient to reverse object valence
- Motion detecting neurons are necessary and sufficient to reverse object valence

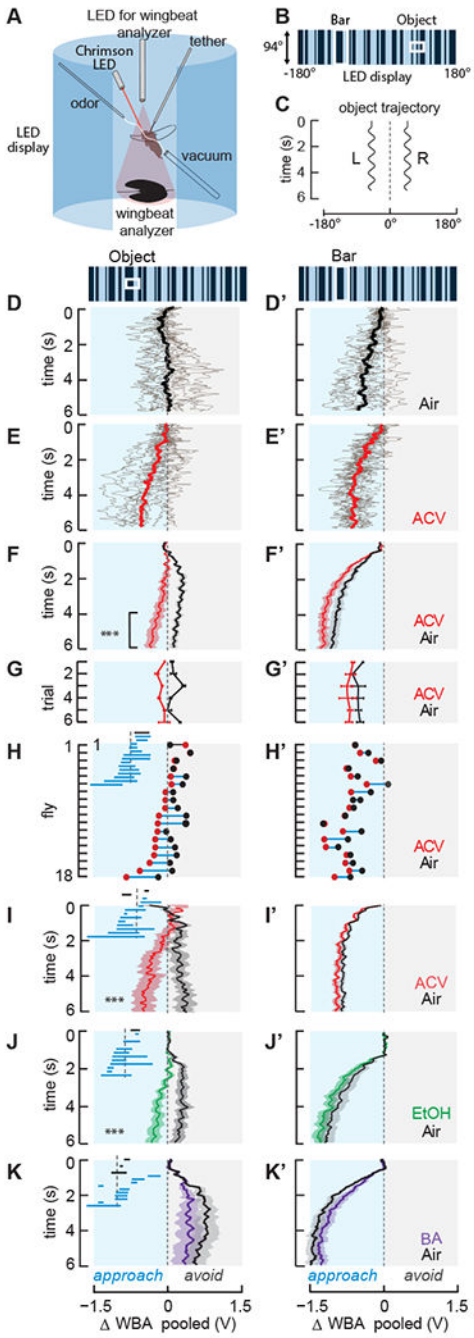

Figure 1. Odor-induced visual valence reversal is odorant specific and learning-independent

(A) Schematic of the rigid-tether visual flight arena equipped for odor delivery and Chrimson optogenetics. The arena is comprised of an array of LED panels controlled by MATLAB. For odor experiments, green panels (570nm) were used, and an odor port was placed in front of the fly. For optogenetics experiments, blue panels (470nm) were used to minimize unwanted Chrimson activation, and a 685nm activating LED was placed in front of the fly. By convention, ΔWBA is defined as left wing beat amplitude (WBA) - right

WBA. ΔWBA<0 corresponds to turning to the left, ΔWBA = 0 corresponds to the fly flying straight or maneuvering in pitch, and ΔWBA>0 corresponds to turning to the right.
(B) Representation of the visual stimuli used in all flight behavior experiments. Random ON-OFF columns comprised both background and object stimuli. A 30×30° square object and 30×94° vertical bar were oscillated sinusoidally at 1Hz.
(C) Stimulus trajectory: ±15° peak-to-peak amplitude centered at ±45° from midline, left or right side selected at random for each trial.
(D,D') Individual repeated trials (gray) by a single fly when each visual stimulus was shown in air, superimposed with the mean ΔWBA response across trials (black). Data from right and left side presentations are inverted and pooled as if all visual stimuli were presented on the left side of the arena. Blue shaded rectangle (negative ΔWBA) indicates when flies are steering toward the visual stimuli ("approach"), and gray rectangle indicate flies steering to "avoid" the stimuli.
(E,E') Same fly as in panel D, with same visual stimuli, in in a plume of ACV. Note valence reversal for the small object (E).
(F,F') Mean ΔWBA (solid line) and SEM (shaded regions) for a population of wild-type PCF flies in response to an object (F) or bar (F') in air (black) or ACV (red). Bracket denotes the final two second epoch used to measure average responses for statistical analysis. Asterisks denote odor-induced visual valence reversal, n=18 $p < 0.01$, Student's paired t-test.
(G,G') Mean ΔWBA and SEM for each consecutive trial, averaged across flies, n=18.
(H,H') Mean ΔWBA of each fly in air (black) and ACV (red), sorted by ΔWBA values. Dots representing mean responses in clean air and ACV from the same fly are joined by a horizontal line. The dots are connected by a blue line for ACV-induced steering shifts toward the visual object and a black line for ACV shifts away from the object. This larger representation demonstrates how we made the inset, which is included in subsequent plots and figures. Inset: same as larger plot, but with dots removed. 12 out of 18 flies shifted their steering effort toward the visual object (blue line) when ACV was presented, and 1 out of 18 steered farther away (black line). Steering responses to the small object that were not influenced by ACV had no segment length value to plot and hence are not indicated, but were included in average points and statistical analyses.
(I,I') Same as row (F) for WT-OregonR flies. Asterisks indicate odor-induced visual valence switch, n=13 *** $p<0.01$.
(J,J') Same as row (F) for ethanol, n=13, *** $p<0.01$.
(K,K') Same as row (F) for an aversive odorant, benzaldehyde, n=14.
See also Figure S1.

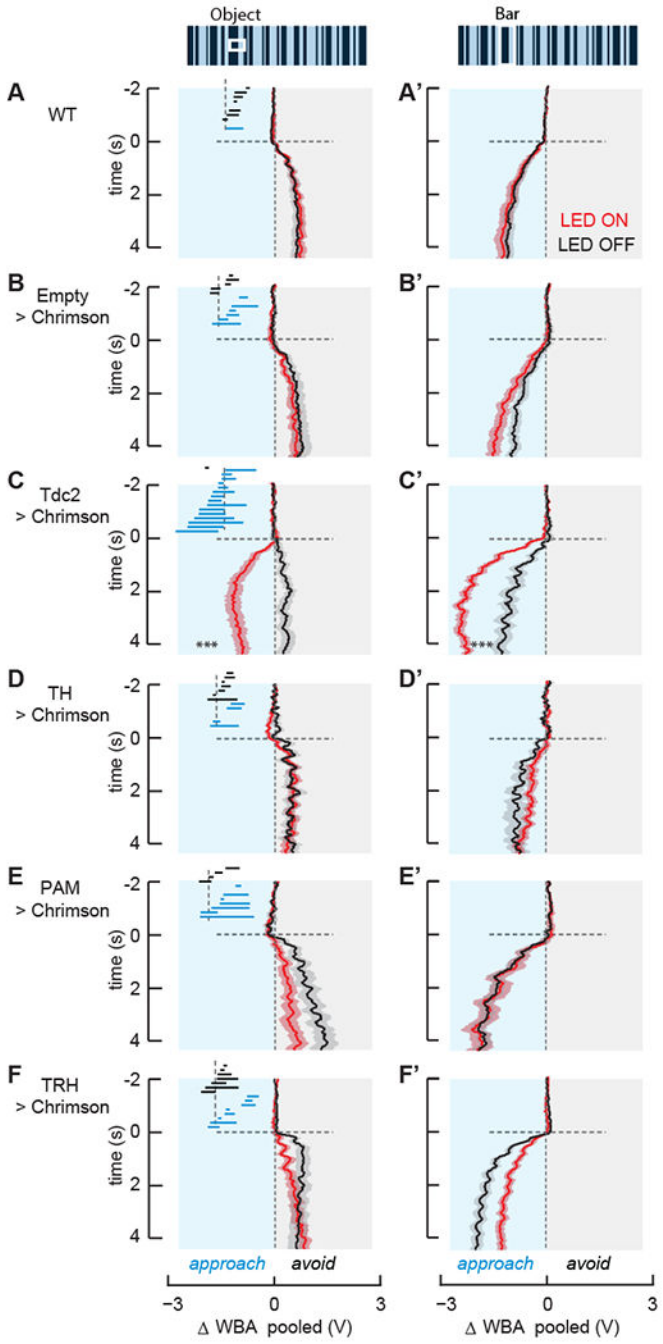

Figure 2. Optogenetic activation of aminergic neurons reveal that OA is sufficient for odor-induced visual valence reversal

All panels - mean ΔWBA (solid lines) and SEM (shaded regions) to an object (A-F) or bar (A'-F') in LED Off (black) or LED On (red) conditions. Each row represents flies of the genotype indicated. In LED On trials, the LED is switched on at time 0. Insets as in Figure 1 denote whether each fly steered more towards (blue) or away from (black) the stimulus upon Chrimson activation. Horizontal dashed line represents the onset of visual stimulus (time = 0). Vertical, dashed gray line represents visual midline (ΔWBA = 0).

(A, A') n=11; (B, B') n=12; (C, C') n=16; (D, D') n=13; (E, E') n=12; (F, F') n=16.

***p<<0.01, Student's paired t-test of the last 2 seconds
See also Figure S2.

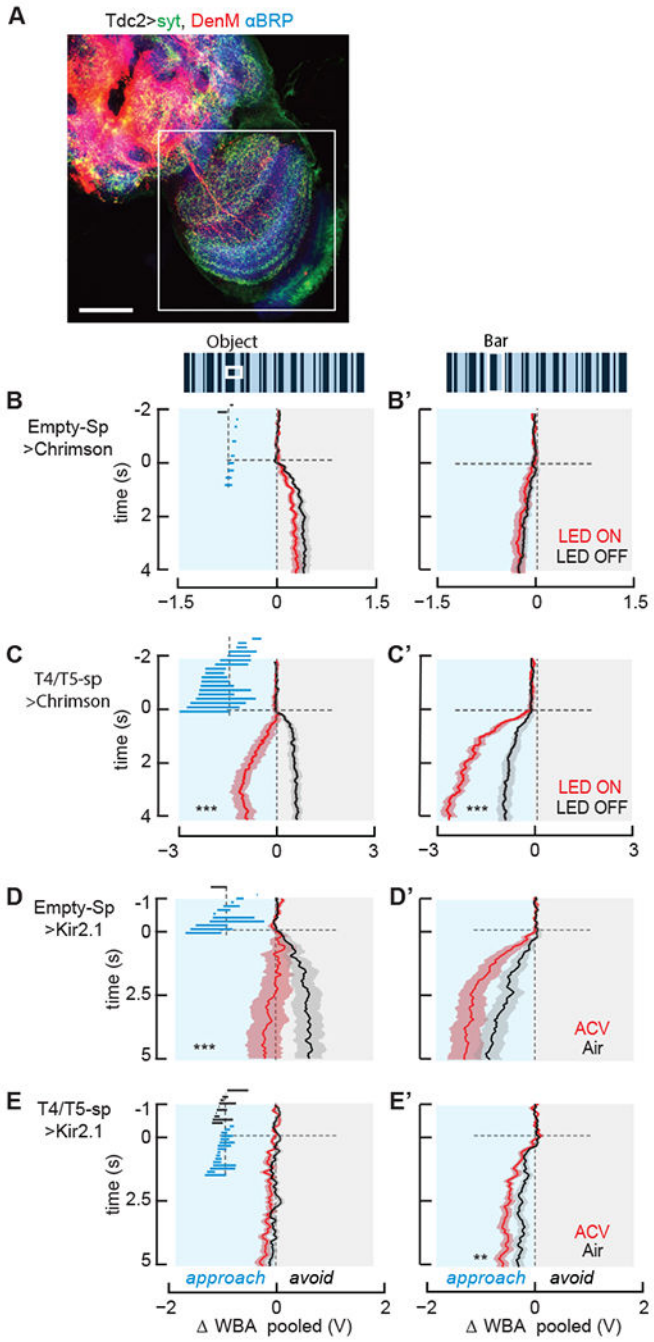

Figure 3. Hyperpolarizing T4/T5 neurons eliminates object responses, depolarizing them induces visual valence reversal

(A) Distribution of presynaptic and dendritic neurites of Tdc2-Gal4 neurons. Red = DenMark labeling; Green = synaptotagmin labeling; Blue = anti-BRP labeling. Me: medulla; Lo: lobula; LoP: lobula plate; SEZ: subesophgeal zone.

(B,B') Genetic controls, enhancerlessless split-gal4 driving UAS-Chrimson, n=19. Mean ΔWBA (solid line) and SEM (shaded region) to an object (B) or bar (B') in LED Off (black) or On (red). Inset: as in Figure 1.

(C,C') Same as B for optogenetic depolarization of T4/T5 neurons, n=18 *** p<<0.01, Student's paired t-test of the last 2 seconds.
(D,D') Genetic controls, enhancerless split-Gal4 driving UAS-Kir2.1, for hyperpolarizing T4/T5 neurons. Mean ΔWBA (solid line) and SEM (shaded region) to an object (D) or bar (D') in clean air (black) or ACV (red) n=13 *** p<<0.01. Inset: as in Figure 1.
(E,E') Same as D, results of hyperpolarizing T4/T5 using Kir2.1, n=27 ** p<0.01, Student's paired t-test of the last 2 seconds.
See also Figure S3.

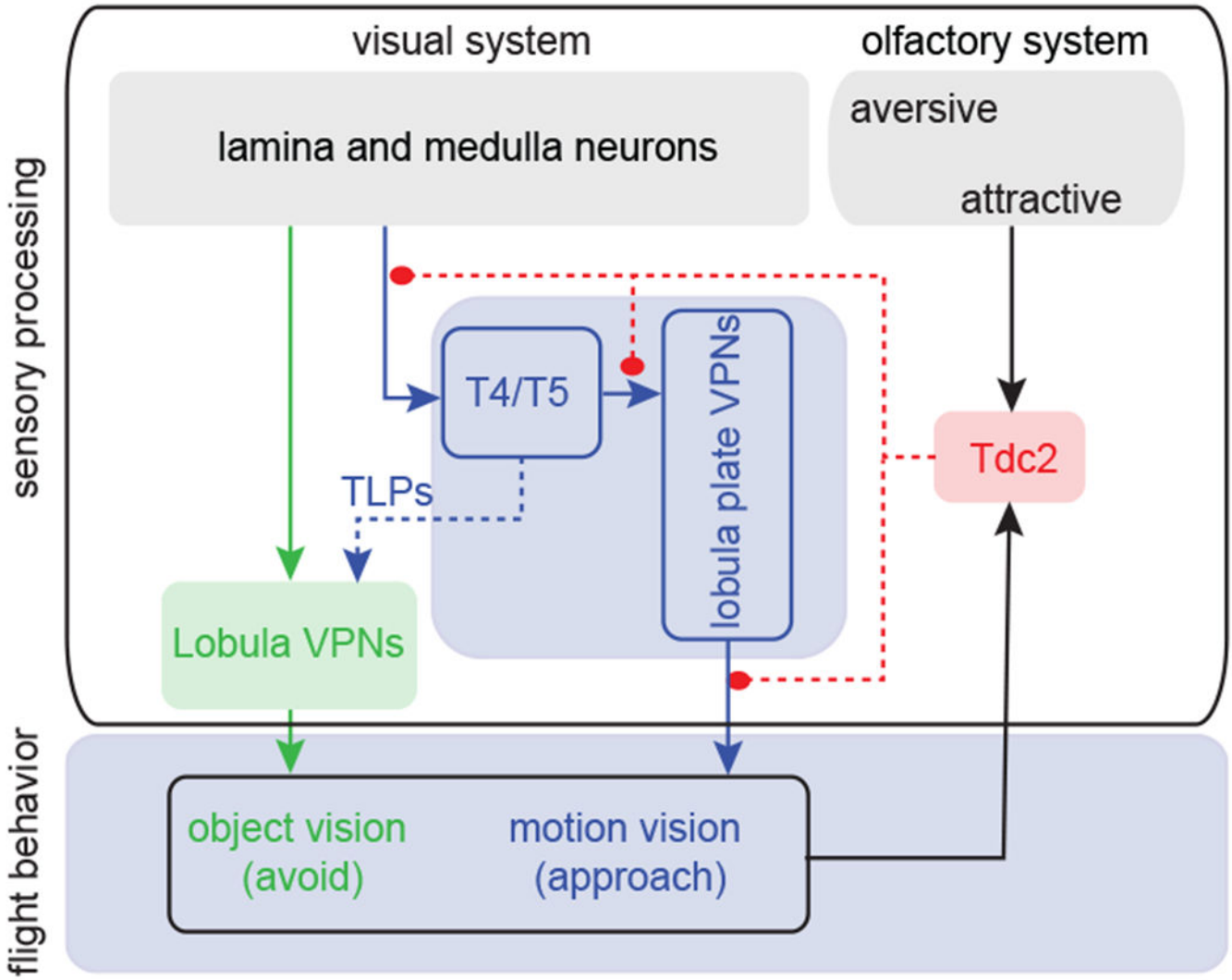

Figure 4. Hypothetical block diagram representing the circuit underlying odor-induced visual valence reversal

Our working model is that olfactory signals act through octopamine signaling to boost the response gain of motion detectors, which in turn elicits robust 'bar like' approach in response to an otherwise weakly aversive small object. Parallel feedforward columnar pathways from the medulla supply object detection via lobula VPNs (green), which combine object and motion signals to mediate weak aversion to small moving objects. Lobula plate VPNs (blue) are also supplied by directionally selective T4/T5 neurons, which are necessary for normal bar approach as well as small object avoidance behaviors - possibly (dashed line) via local translobula plate interneurons (TLPs). In flight, T4/T5 optogenetic activation is sufficient to elicit visual object valence reversal. The onset of flight behavior combines with attractive odor signals to activate Tdc2 neurons (red), which release octopamine. To date, evidence shows that octopamine modulates (filled circles) all components of the motion vision circuit, but exactly where in the circuit is unknown (dashed lines). In flight, optogenetic activation of Tdc2 is sufficient to elicit visual object valence reversal.

KEY RESOURCES TABLE

REAGENT or RESOURCE	SOURCE	IDENTIFIER
Antibodies		
Mouse anti-Bruchpilot (nc82)	Developmental Studies Hybridoma Bank	nc82; RRID: AB_2314866
Rabbit anti-dsRed	Clontech	632496
Chicken anti-GFP	Abcam	RRID: AB_13970
AlexaFluor647-Donkey anti-Mouse IgG	Jackson Immuno Research Libraries, Inc.	715-605-150
AlexaFluor568 Goat anti-Rabbit IgG(H+L)	Fisher Scientific	A11036
AlexaFluor488 Goat anti-Chicken IgY	Abcam	RRID: AB_150169
Chemicals		
benzaldehyde	Sigma-Aldrich	B1334
ethanol	Decon Laboratories	N/A
All-trans retinal	Sigma Aldrich	R2500
Electronic Equipment		
LED panels visual display system	N/A	[16]
8×8 dot matrix LED panels	Adafruit	470nm, 570nm
Photoionization detector	Aurora Scientific	miniPID 200B
Neurtral density optical filter	Rosco	Cat#59
Wingbeat analyzer	JFI Electronics	N/A
Experimental Models: Organisms/Strains		
D. melanogaster: Tdc2-Gal4	Bloomington Drosophila Stock Center	RRID: BDSC_9313
D. melanogaster: TH-Gal4	Bloomington Drosophila Stock Center	RRID: BDSC_8848
D. melanogaster: TRH-Gal4	Gift from S.Birman lab	N/A
D. melanogaster: Empty-Gal4 (pBDPGal4U)	[34]	N/A
D. melanogaster: Empty split-Gal4 (pBPp65ADZpUw; pBPZpGAL4DBDUw)	Janelia Research Campus	N/A
D. melanogaster:SS00324-SplitGal4 R59E0_AD (attP40); R42F06_DBD(attP2)	Janelia Research Campus	N/A
D. melanogaster: 20×UAS-Chrimson::tdTomato-VK5	Gift from D. Anderson lab	N/A
D. melanogaster: w^{1118}; UAS-DenMark, UAS-syt.eGFP; D^{1}/TM6C	Bloomington Drosophila Stock Center	RRID: BDSC_33064
w+(DL);;pJFRC49-10XUAS-IVS-eGFP-Kir2.1	[74]	N/A
D. melanogaster OregonR wild-type flies		N/A
D. melanogaster population cage flies, reared from wild-caught iso-female line, originally from Michael Dickinson's lab	Frye lab	DL
Software and Algorithms		
MATLAB 2017a	Mathworks, Inc.	N/A
Fiji (ImageJ)	NIH	N/A